BOUNDARY-ROUGHNESS EFFECTS IN NEMATIC LIQUID CRYSTALS

PAOLO BISCARI AND STEFANO TURZI*

Abstract. We study the equilibrium configuration of a nematic liquid crystal bounded by a rough surface. The wrinkling of the surface induces a partial melting in the degree of orientation. This softened region penetrates the bulk up to a length scale which turns out to coincide with the characteristic wave length of the corrugation. Within the boundary layer where the nematic degree of orientation decreases, the tilt angle steepens and gives rise to a nontrivial structure, that may be interpreted in terms of an effective weak anchoring potential. We determine how the effective surface extrapolation length is related to the microscopic anchoring parameters. We also analyze the crucial role played by the boundary conditions assumed on the degree of orientation. Quite different features emerge depending on whether they are Neumann- or Dirichlet-like. These features may be useful to ascertain experimentally how the degree of orientation interacts with an external boundary.

Key words. Nematic liquid crystals, surface roughness, surface melting, weak anchoring

AMS subject classifications. 76A15, 74A50, 82D30

Nematic liquid crystals are fluid aggregates of elongated molecules. When the nematic rods interact with an external surface, the elastic strain energy induces them to align parallel to the unit normal, even if the surface is not perfectly flat [1]. Recent experimental observations confirm that the surface alignment of the nematic director is completely determined by the roughness-induced surface anisotropy [2]. Further analytical calculations, performed within the classical Frank model with unequal elastic constants, have detected the bulk effects induced by a periodically-modeled external boundary [3].

A crucial effect, still related to surface roughness, escapes the framework of Frank theory, where the only order parameter is the director. Indeed, it is physically intuitive that nematic molecules will disorder if we force them to follow a rapidly varying boundary condition. This *surface melting* was first experimentally detected in [4, 5]. Recent experimental observations have also measured a boundary-layer structure in the degree of orientation [6]. The surface melting has been confirmed by approximated analytical solutions [7], numerical calculations [8, 9], and molecular Monte-Carlo simulations [10].

The combined effect of a rapidly-varying director anchoring and surface melting gives rise to an effective weak-anchoring effect that was first observed in [11]. The problem of relating the effective anchoring extrapolation length to the microscopic roughness parameters has been studied in several theoretical papers, all framed within the Frank theory [12, 13, 14]. This observation is of basic significance, since weak anchoring potentials have proven to influence deeply all nematic phenomena, beginning with Freedericksz transitions [15, 16, 17]. Indeed, several theoretical studies have already determined the influence on anchoring energies of the presence of permanent surface dipoles [18] or diluted surface potentials [19, 20].

In this paper we analyze in analytical detail the boundary-layer structure induced by a rough surface which bounds a nematic liquid crystal. We frame within the Landau-de Gennes order-tensor theory, to be able to detect the effects on both the director and the degree of orientation. Our results confirm the surface melting already

*Dipartimento di Matematica, Politecnico di Milano, Piazza Leonardo da Vinci 32, 20133 Milano (Italy). E-mail: `paolo.biscari@polimi.it`, `stefano.turzi@mate.polimi.it`

obtained in [7], but allow us to detect new phenomena. First, the nematic director steepens close to the boundary, so giving rise to an effective weak anchoring potential, that turns out to be deeply related to the surface-melting effect, and thus can be correctly handled only within the order-tensor theory. Furthermore, the boundary layers display a strong dependence on the type of boundary conditions imposed on the degree of orientation. Indeed, the orders of magnitude of all the expected effects depend on whether the boundary conditions are Neumann- or Dirichlet-like. We discuss how these effects may help in ascertaining in experiments how the mesoscopic parameter, which measures he degree of order, interacts with an external surface.

The paper is organized as follows. In Section 1 we present the model, we set the geometry of a roughly-bounded sample, and derive the Euler-Lagrange partial differential equations that determine the equilibrium configurations. In Section 2 we perform the perturbative two-scales analysis that provides all the analytical details of the boundary-layer structure. In Section 3 we solve an effective problem, in which the rough surface is replaced by a weak-anchoring potential. The concluding Section 4 compares our outcomes with the effective results of Section 3, and draws the conclusions.

1. Equilibrium configurations. The degree of order decrease has been recognized by many authors as a crucial effect of surface roughness [7, 9]. We thus describe nematic configurations in the framework of the Landau-de Gennes **Q**-tensor theory [21]. The order tensor is defined as the deviatoric part of the second-moment of the probability distribution of molecular orientations:

$$\mathbf{Q}(\mathbf{r}) := \int_{\mathbb{S}^2} (\mathbf{m} \otimes \mathbf{m}) \, f_r(\mathbf{m}) \, da - \frac{1}{3} \, \mathbf{I} \,, \tag{1.1}$$

where **I** denotes the identity tensor. **Q** is a second-order traceless symmetric tensor, with $\mathrm{sp}\,\mathbf{Q} \subset \left[-\frac{1}{3}, \frac{2}{3} \right]$ [16].

In order to keep computations simple, we adopt the one-constant approximation for the elastic part of the free energy functional

$$f_{\mathrm{el}}[\mathbf{Q}] = \frac{1}{2} \, K \, |\nabla \mathbf{Q}|^2 \,, \tag{1.2}$$

where K is an average elastic constant. We stress, however, that it is straightforward to generalize all what follows to take into account unequal material elastic constants.

The free-energy functional includes the Landau-de Gennes thermodynamic potential as well

$$f_{\mathrm{LdG}}(\mathbf{Q}) = A \, \mathrm{tr}\,\mathbf{Q}^2 - B \, \mathrm{tr}\,\mathbf{Q}^3 + C \, \mathrm{tr}\,\mathbf{Q}^4 \,. \tag{1.3}$$

The material parameter A depends on the temperature, and in particular it becomes negative deep in the nematic phase. On the contrary, B, C can be assumed to be positive and temperature-independent. The potential (1.3) strongly favors uniaxial phases, in which at least two of the three eigenvalues of **Q** coincide. In fact, **Q** is expected to abandon uniaxiality mainly close to director singularities [22, 23, 24]. We will not deal with any defect structure. Thus, though the uniaxiality constraint is not essential for our purposes, we follow the attitude of avoiding unnecessary complications [25, 26], and restrict our attention to uniaxial states

$$\mathbf{Q}(\mathbf{r}) = s(\mathbf{r}) \left(\mathbf{n}(\mathbf{r}) \otimes \mathbf{n}(\mathbf{r}) - \frac{1}{3} \, \mathbf{I} \right) \,. \tag{1.4}$$

The scalar $s \in \left[-\frac{1}{2}, 1\right]$ and the unit vector $\mathbf{n}$ are respectively the *degree of orientation* and the *director*. With the aid of (1.4), the potentials (1.2),(1.3) can be written as

$$f_{\text{el}}[s, \mathbf{n}] = K\left(s^2|\nabla\mathbf{n}|^2 + \tfrac{1}{3}|\nabla s|^2\right) \quad \text{and} \quad f_{\text{LdG}}(s) = \tfrac{2}{3}A\,s^2 - \tfrac{2}{9}B\,s^3 + \tfrac{2}{9}C\,s^4 \; . \quad (1.5)$$

When $A \leq B^2/(12C)$, the absolute minimum of the function $f_{\text{LdG}}(s)$ occurs at the *preferred degree of orientation*

$$s_{\text{pr}} := \frac{3B + \sqrt{9B^2 - 96AC}}{8C} > 0 \; . \quad (1.6)$$

In order to gain physical interpretation of the results, we also introduce the *nematic coherence length* ξ and the dimensionless (positive) parameter ω, defined as

$$\xi^2 := \frac{9K}{C} \qquad \text{and} \qquad \omega^2 := \frac{2}{3}\left(s_{\text{pr}}B - 4A\right) \; . \quad (1.7)$$

The nematic coherence length compares the strength of the elastic and thermodynamic contributions to the free energy functional. We will show below that it characterizes the size of the domains where the degree of orientation may abandon its preferred value s_{pr}. The number ω depends on the depth of the potential well associated with s_{pr}. Indeed, it is defined in such a way that $f''_{\text{LdG}}(s_{\text{pr}}) = \omega^2/\xi^2$.

By using (1.6),(1.7) we write the bulk free-energy density $f_{\text{b}} := f_{\text{el}} + f_{\text{LdG}}$ as

$$\frac{f_{\text{b}}[s, \mathbf{n}]}{K} = s^2|\nabla\mathbf{n}|^2 + \frac{1}{3}|\nabla s|^2 + \frac{1}{\xi^2}\left(s^4 - \frac{4}{3}s^3\left(2s_{\text{pr}} - \frac{\omega^2}{s_{\text{pr}}}\right) + 2s^2(s_{\text{pr}}^2 - \omega^2)\right) . \quad (1.8)$$

1.1. Modelling a rough surface. We aim at analyzing the effects that a rough boundary induces in a nematic liquid crystal. Once again, we try to keep our analysis as simple as possible, while still catching the essential features. We thus follow *e.g.* [12] in modeling roughness by imposing a sinusoidally-perturbed homeotropic anchoring condition on a flat surface. The amplitude and the wave length characterizing the perturbation will be the crucial parameters in our results.

We focus attention on a thin boundary layer, attached to the external surface. Consequently, we disregard the detailed structure of the bulk equilibrium configuration, that will only enter our results as asymptotic *outer* solution for the surface boundary layer. We introduce a Cartesian frame of reference $\{\mathbf{e}_x, \mathbf{e}_y, \mathbf{e}_z\}$, and assume that the nematic spreads in the whole half-space $\mathcal{B} = \{z \geq 0\}$. We further simplify the geometry by assuming that $\mathbf{n}(\mathbf{r}) = \sin\theta(\mathbf{r})\,\mathbf{e}_x + \cos\theta(\mathbf{r})\,\mathbf{e}_z$ and that the asymptotic bulk configuration depends only on z

$$\theta(\mathbf{r}) \approx \theta_{\text{b}}(z) \qquad \text{as} \quad z \to +\infty \; . \quad (1.9)$$

In the presence of strong homeotropic anchoring on a flat surface, the boundary condition to be imposed on the director would be $\theta^{(\text{flat})}(x, y, 0) = 0$. On the contrary, we will require

$$\theta(x, y, 0) = \Delta\cos\frac{x}{\eta} \; . \quad (1.10)$$

The boundary condition (1.10) mimics the rugosity of the external surface by introducing two new parameters: the (dimensionless) roughness amplitude Δ and the roughness length η. We remark that the oscillation rate increases as $\eta \to 0^+$, while

all roughness effects are expected to vanish in the limit $\Delta \to 0^+$. The requirements (1.9),(1.10) imply that the free-energy minimizer will not exhibit any dependence on the transverse y-coordinate, so that we will henceforth restrict attention to the dependence on the coordinates (x, z).

It is more complex to ascertain the correct type of boundary conditions which are to be imposed on the degree of orientation s. From the mathematical point of view, it would be natural to imitate the (Dirichlet) strong anchoring imposed on the director, and thus set $s(x, y, 0)$ to be equal to some fixed boundary value $\tilde{s}$. Nevertheless, while it is well-established that we can induce an easy axis for the director on an external boundary, it is questionable whether we may fix the value of a mesoscopic parameter, that measures the degree of order in a distribution. From the physical point of view it would appear then more natural to impose (Neumann) free boundary conditions on the degree of orientation, leaving to the thermodynamic potential (1.3) the assignment of inducing the preferred value s_{pr} in the bulk ($z \to \infty$). To be safe, both possibilities (Dirichlet and Neumann) will be analyzed in Section 2.

1.2. Euler-Lagrange equations. Once we consider that $|\nabla \mathbf{n}|^2 = |\nabla \theta|^2$, it is easy to derive the Euler-Lagrange partial differential equations associated with the functional (1.8). They read:

$$s^2 \Delta \theta + 2\, s\, \nabla s \cdot \nabla \theta = 0 \qquad \text{and} \qquad \Delta s - 3\, s\, |\nabla \theta|^2 - 3\, \frac{\sigma(s)}{\xi^2} = 0\,, \qquad (1.11)$$

where

$$\sigma(s) := s(s - s_{\mathrm{pr}}) \left(s - s_{\mathrm{pr}} + \frac{\omega^2}{s_{\mathrm{pr}}} \right)\,. \qquad (1.12)$$

Since the boundary conditions (1.10) are x-periodic, with a period of $2\pi\eta$, we look for solutions of (1.11) in $C^2_{2\pi\eta}$ (the space of C^2-functions, $2\pi\eta$-periodic in the x-direction). To complete the differential system (1.10), in §2.1 we will require

$$\begin{cases} \theta(x, 0) = \Delta \cos \dfrac{x}{\eta} \\ \dfrac{\partial s}{\partial z}(x, 0) = 0 \end{cases} \qquad \text{and} \qquad \begin{cases} \theta(x, z) \approx \theta_{\mathrm{b}}(z) \\ s(x, z) \approx s_{\mathrm{pr}} \end{cases} \qquad \text{as } z \to \infty \qquad (1.13)$$

while in §2.2 we will choose

$$\begin{cases} \theta(x, 0) = \Delta \cos \dfrac{x}{\eta} \\ s(x, 0) = \tilde{s} \end{cases} \qquad \text{and} \qquad \begin{cases} \theta(x, z) \approx \theta_{\mathrm{b}}(z) \\ s(x, z) \approx s_{\mathrm{pr}} \end{cases} \qquad \text{as } z \to \infty \qquad (1.14)$$

2. Two-scales analysis. Before proceeding with the perturbation analysis of the differential equations, we state them in dimensionless form. It will turn out that the correct scaling is obtained by measuring lengths in η-units, so that we introduce the new dimensionless coordinates $\bar{x} = x/\eta$, $\bar{z} = z/\eta$, and define the dimensionless parameter $\varepsilon = \xi/\eta$. Equations (1.11) become thus

$$s^2 \Delta \theta + 2s\, \nabla s \cdot \nabla \theta = 0 \qquad \text{and} \qquad \varepsilon^2 \Delta s - 3\varepsilon^2 s\, |\nabla \theta|^2 - 3\sigma(s) = 0\,, \qquad (2.1)$$

where both the gradient and the laplacian are now to be intended with respect to the scaled variables. The nematic coherence length is usually much smaller than all other

characteristic lengths. Consequently, we will look for uniformly asymptotic solutions to (2.1), by treating ε as a small parameter. In this limit, equation $(2.1)_2$ is singular, so that a regular asymptotic expansion would not provide a uniform approximation of the solution. Indeed, the small parameter ε multiplies the highest derivative, so that we may expect the solution to have a steep behavior in a layer of thickness δ (to be determined), close to the boundary $z = 0$. We refer the reader to the books [27, 28, 29, 30] for the details of the singular perturbation theory we will apply henceforth and, in particular, for the technique of the two-scales method which directly yields a uniform approximation of the solution.

A standard dominant balance argument (that requires to introduce a stretched variable $Z = \bar{z}/\delta$) allows to recognize that the boundary layer thickness is $\delta = \varepsilon$. We then introduce the *fast* variable $Z = \bar{z}/\varepsilon$. The two-scales chain rule requires to replace $\partial_{\bar{z}}$ by $\left(\partial_{\bar{z}} + \varepsilon^{-1}\partial_Z\right)$, and equations (2.1) take the form (when $s \neq 0$)

$$s\left(\varepsilon^2\theta_{,\bar{x}\bar{x}} + \varepsilon^2\theta_{,\bar{z}\bar{z}} + 2\varepsilon\theta_{,\bar{z}Z} + \theta_{,ZZ}\right) + 2\varepsilon^2 s_{,\bar{x}}\theta_{,\bar{x}} + 2(\varepsilon s_{,\bar{z}} + s_{,Z})(\varepsilon\theta_{,\bar{z}} + \theta_{,Z}) = 0 \quad (2.2)$$

$$\varepsilon^2 s_{,\bar{x}\bar{x}} + \varepsilon^2 s_{,\bar{z}\bar{z}} + 2\varepsilon s_{,\bar{z}Z} + s_{,ZZ} - 3s\left[\varepsilon^2(\theta_{,\bar{x}})^2 + (\varepsilon\theta_{,\bar{z}} + \theta_{,Z})^2\right] - 3\sigma(s) = 0 \quad (2.3)$$

where a comma denotes differentiation with respect to the indicated variable. In agreement with the two-scales method, θ and s are now to be intended as $\theta(\bar{x}, \bar{z}, Z)$ and $s(\bar{x}, \bar{z}, Z)$, that is functions of $\bar{x}, \bar{z}$ and Z regarded as *independent* variables. It will be only at the very end of our calculations that we will recast the connection between $\bar{z}$ and Z: $Z = \bar{z}/\varepsilon$. We seek for solutions which may be given the formal expansions

$$\theta(\bar{x}, \bar{z}, Z) = \theta_0(\bar{x}, \bar{z}, Z) + \varepsilon\theta_1(\bar{x}, \bar{z}, Z) + \varepsilon^2\theta_2(\bar{x}, \bar{z}, Z) + O(\varepsilon^3) \quad (2.4)$$

$$s(\bar{x}, \bar{z}, Z) = s_0(\bar{x}, \bar{z}, Z) + \varepsilon s_1(\bar{x}, \bar{z}, Z) + \varepsilon^2 s_2(\bar{x}, \bar{z}, Z) + O(\varepsilon^3) . \quad (2.5)$$

If we insert (2.4)-(2.5) in (2.2)-(2.3), we obtain the following sequence of differential equations to $\mathcal{O}(1)$, $\mathcal{O}(\varepsilon)$, and $\mathcal{O}(\varepsilon^2)$

$$\begin{cases} \frac{1}{s_0}\left(s_0^2\theta_{0,Z}\right)_{,Z} = 0 \\ s_{0,ZZ} - 3s_0(\theta_{0,Z})^2 - 3\sigma(s_0) = 0 \end{cases} \quad (2.6)$$

$$\begin{cases} \frac{1}{s_0}\left(s_0^2\theta_{1,Z}\right)_{,Z} + \frac{1}{s_1}\left(s_1^2\theta_{0,Z}\right)_{,Z} = -2\left(s_0\theta_{0,Z}\right)_{,\bar{z}} - 2s_{0,Z}\theta_{0,\bar{z}} \\ s_{1,ZZ} - 6s_0\theta_{0,Z}\theta_{1,Z} - 3s_1\left(\sigma'(s_0) + (\theta_{0,Z})^2\right) = 6s_0\theta_{0,Z}\theta_{0,\bar{z}} - 2s_{0,\bar{z}Z} \end{cases} \quad (2.7)$$

$$\begin{cases} \frac{1}{s_0}(s_0^2\theta_{2,Z})_{,Z} + \frac{1}{s_2}(s_2^2\theta_{0,Z})_{,Z} = -\frac{1}{s_1}(s_1^2\theta_{1,Z})_{,Z} - \frac{1}{s_0}(s_0^2\theta_{0,\bar{z}})_{,\bar{z}} - \frac{1}{s_0}(s_0^2\theta_{0,\bar{x}})_{,\bar{x}} \\ \qquad - 2\left(s_0\theta_{1,Z}\right)_{,\bar{z}} - 2\left(s_1\theta_{0,Z}\right)_{,\bar{z}} - 2s_{1,Z}\theta_{0,\bar{z}} - 2s_{0,Z}\theta_{1,\bar{z}} \\ s_{2,ZZ} - 3s_2\left[\sigma'(s_0) + (\theta_{0,Z})^2\right] - 6s_0\theta_{0,Z}\theta_{2,Z} = \frac{3}{2}s_1^2\sigma''(s_0) \\ \qquad + 3s_0\left[(\theta_{0,\bar{z}} + \theta_{1,Z})^2 + (\theta_{0,x})^2\right] \\ \qquad + 6\theta_{0,Z}\left(s_1\theta_{1,Z} + s_1\theta_{0,\bar{z}} + s_0\theta_{1,\bar{z}}\right) - 2s_{1,\bar{z}Z} - s_{0,\bar{z}\bar{z}} - s_{0,xx} . \end{cases} \quad (2.8)$$

Analogous equations can be easily derived at any desired order. For any $n \geq 1$, the differential system obtained at $\mathcal{O}(\varepsilon^n)$ is linear in the unknowns θ_n, s_n, and may be solved analytically. By virtue of the multiscale method, we find the correct dependence on $\bar{z}, Z$ by requiring that all s_n, θ_n are uniformly bounded as $\varepsilon \to 0^+$ for expanding intervals of the type $0 \leq Z \leq Z^*/\varepsilon$, for a suitable positive constant Z^*. In most practical cases this requirement is equivalent to asking the removal of secular terms (*i.e.* terms that diverge as $Z \to +\infty$).

2.1. Free surface degree of orientation. In terms of the scaled variables, the boundary conditions (1.13) require

$$\begin{cases} \theta(\bar{x},0) = \Delta \cos \bar{x} \\ s_{,\bar{z}}(x,0) = 0 \end{cases} \quad \text{and} \quad \begin{cases} \theta(\bar{x},\bar{z}) \approx \theta_{\mathrm{b}}(\eta \bar{z}) \\ s(\bar{x},\bar{z}) \approx s_{\mathrm{pr}} \end{cases} \quad \text{when } \bar{z} \gg \eta . \qquad (2.9)$$

We introduce $\mathrm{m} := \theta_{\mathrm{b}}'(0)$, the derivative of the asymptotic solution at $z = 0$, since it will play an important role in the following discussion. The leading solutions in expansions (2.4),(2.5) are

$$s_0(x,z) = s_{\mathrm{pr}} \quad \text{and} \quad \theta_0(x,z) = \mathrm{m}\, z + \Delta \mathrm{e}^{-z/\eta} \cos \frac{x}{\eta} . \qquad (2.10)$$

Higher order asymptotic solutions are gathered by means of laborious but straightforward calculations. After recasting the solutions in terms of the dimensional variables $x = \eta \bar{x}$ and $z = \eta \bar{z}$, we find

$$s(x,z) = s_{\mathrm{pr}} - \frac{s_{\mathrm{pr}}\xi^2}{\omega^2} \left(\mathrm{m}^2 - \frac{2\,\mathrm{m}\,\Delta}{\eta} \mathrm{e}^{-z/\eta} \cos \frac{x}{\eta} + \frac{\Delta^2}{\eta^2} \mathrm{e}^{-2z/\eta} \right)$$

$$+ \frac{2 s_{\mathrm{pr}}\,\xi^3}{\sqrt{3}\,\omega^3} \mathrm{e}^{-\sqrt{3}\omega z/\xi} \left(\frac{\Delta^2}{\eta^3} - \frac{\mathrm{m}\,\Delta}{\eta^2} \cos \frac{x}{\eta} \right) + \mathcal{O}\left(\varepsilon^4 \right) \quad \text{and} \qquad (2.11)$$

$$\theta(x,z) = \mathrm{m}\, z + \Delta\, \mathrm{e}^{-z/\eta} \cos \frac{x}{\eta} + \frac{\xi^2}{\omega^2} \left(\frac{2\,\mathrm{m}\,\Delta^2}{\eta} \left(1 - \mathrm{e}^{-2z/\eta} \right) \right.$$

$$\left. - \frac{\Delta^3}{2\,\eta^2} \left(\mathrm{e}^{-z/\eta} - \mathrm{e}^{-3z/\eta} \right) \cos \frac{x}{\eta} - \frac{2\,\mathrm{m}^2\,\Delta}{\eta} z\, \mathrm{e}^{-z/\eta} \cos \frac{x}{\eta} \right) + \mathcal{O}\left(\varepsilon^4 \right) . \qquad (2.12)$$

The above expansions have been carried out up to the first nontrivial correction of the 0th-order approximation. Indeed, all calculations must be pushed to $\mathcal{O}\left(\varepsilon^3 \right)$ since an internal ξ-layer is necessary to satisfy the boundary condition (1.13) in $z = 0$. This layer is of $\mathcal{O}\left(\varepsilon^3 \right)$ because in the Neumann case the boundary condition (1.13) concerns the first derivative of s, instead of the degree of orientation itself. We remark that the solutions (2.11)-(2.12) are coherently ordered for every fixed value of $\eta \neq 0$. However, they are not uniformly ordered when $\eta \in (0,\bar{\eta}]$, namely we don't have a uniform solution if η is allowed to become of order ξ or, still worse, tend to zero. In other words, the above solutions remain valid as $\eta \to 0^+$ if and only if $\xi = o\left(\eta\right)$. The main properties of the equilibrium configurations in the mathematically appealing but physically uncommon case in which η is of the order of, or even smaller than, ξ will be presented elsewhere [31].

2.1.1. Surface melting. We can highlight three different contributions in the degree of orientation (2.11). First, we notice a uniform decrease in the degree of order, equal to $-s_{\mathrm{pr}}\mathrm{m}^2\xi^2/\omega^2$. This disordering effect is triggered by the θ-derivative m, and was certainly to be expected. In fact, a glance to the free energy functional (1.8) suffices to show that a reduction in s decreases the free energy whenever the gradient of the director is not null. We then find two boundary layers. The former, of thickness η and $\mathcal{O}\left(\varepsilon^2 \right)$, is a further reduction of the degree of orientation due to the boundary roughness, that induces a director variation in the x-direction. An internal boundary layer, of thickness ξ and order $\mathcal{O}\left(\varepsilon^3 \right)$, is finally needed in order to cancel the normal derivative of s at the external surface. If we take into account all the contributions, the mean surface degree of orientation, defined as the x-average of $s(x,0)$, turns out

to be

$$< s(x,0) >_x = s_{\mathrm{pr}} \left[1 - \frac{\mathrm{m}^2 \xi^2}{\omega^2} - \frac{\Delta^2 \xi^2}{\omega^2 \eta^2} + \frac{2 \Delta^2 \xi^3}{\sqrt{3}\, \omega^3 \eta^3} \right] \; . \tag{2.13}$$

Figure 2.1 evidences the reported behaviour of the mean degree of orientation as a function of the distance from the surface.
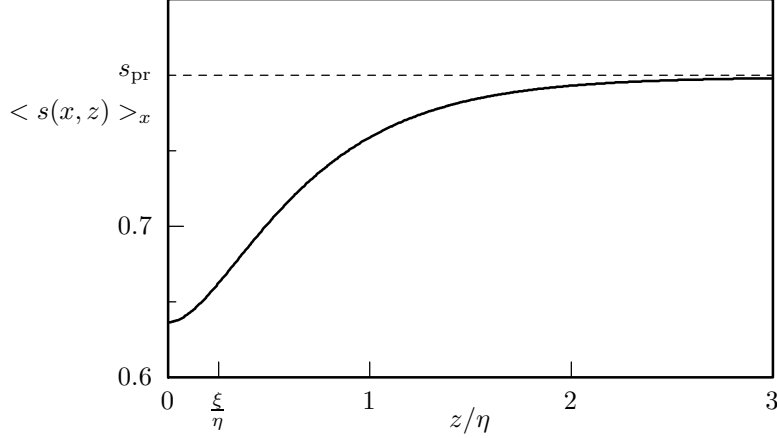

FIG. 2.1. *Boundary layers in the mean degree of orientation* $< s(x,z) >_x$, *when* $\xi = 0.25\eta$, $s_{\mathrm{pr}} = 0.8$, $\omega = 0.6$, $\mathrm{m} = 0.1/\eta$, *and* $\Delta = 1.5$. *The plot exhibits the presence of* two *boundary layers, the internal one being required by the free boundary condition applied on s.*

2.1.2. Effective surface angle. The tilt angle θ exhibits a boundary-layer structure as well. Equation (2.12) shows that such layer is of $\mathcal{O}\left(\varepsilon^2\right)$ and thickness η. It gives rise to an interesting effective misalignment of the surface director. Indeed, if we allow $z \gg \eta$ in (2.12) we find that

$$\theta(x,z) \approx \theta_{\mathrm{b}}(z) = \frac{2\,\mathrm{m}\,\xi^2 \Delta^2}{\eta \omega^2} + \mathrm{m}\,z \qquad \text{as} \quad z \gg \eta \; . \tag{2.14}$$

The asymptotic approximation (2.14) shows that an experimental observation, performed sufficiently far from the external plate (with respect to the microscopic scale η) would detect an *effective* tilt angle θ_{b}, whose value at the plate is different from zero, since

$$\theta_{\mathrm{b}}(0) = \frac{2\,\mathrm{m}\,\xi^2 \Delta^2}{\eta \omega^2} \; . \tag{2.15}$$

Thus, a coarse observation of the nematic configuration measures a surface tilt angle slightly different from the homeotropic prescription $\theta_{\mathrm{surf}} = 0$. Figure 2.2 evidences this effect. In the next section we will analyze in more detail the result (2.15). Then we will show how it matches the predictions of an effective weak anchoring potential. We remark that the tilt angle does not exhibit any further boundary layer at the smaller scale ξ.

2.2. Fixed surface degree of orientation. The perturbative analysis of the differential equations (1.11), with the Dirichlet boundary conditions (1.14), would be unnecessarily entangled because of the non-linearity of the thermodynamic potential
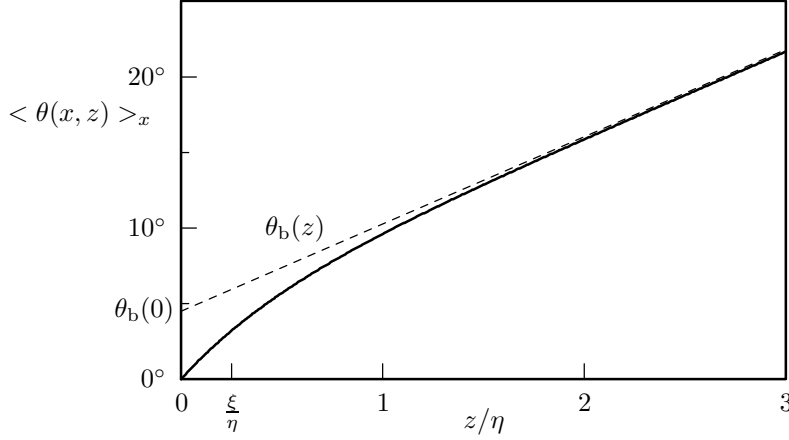
FIG. 2.2. *Boundary layer in the mean tilt angle* $< \theta(x,z) >_x$, *when* $\xi = 0.25\eta$, $s_{\mathrm{pr}} = 0.8$, $\omega = 0.6$, $\mathrm{m} = 0.1/\eta$, *and* $\Delta = 1.5$. *The dashed line corresponds to the asymptotic, linear approximation* $\theta_{\mathrm{b}}(z)$.

(1.12). In fact, in this case only implicit solutions for $s_0(x,z,Z)$ can be gathered. In order to pursue our analysis, and still catch the essential features of the solutions, we replace the function σ in (1.11) by its linear approximation $\sigma_1(s) = \omega^2(s - s_{\mathrm{pr}})$. This is tantamount to replacing the Landau-de Gennes potential in (1.5) by a tangent quadratic well, still centered in s_{pr}. Such approximation is certainly well-justified deep in the nematic phase, when the isotropic state $s = 0$ becomes unstable, and the second well of the Landau-de Gennes potential can be neglected.

The asymptotic properties of the solutions in this case depend critically on the value $\tilde{s}$ forced on the surface. If $\tilde{s} \neq s_{\mathrm{pr}}$, the boundary layer induced by the Dirichlet condition dominates over the roughness effect. Indeed, the leading asymptotic solutions are given by

$$
\begin{aligned}
s(x,z) = s_{\mathrm{pr}} &- (s_{\mathrm{pr}} - \tilde{s})\, \mathrm{e}^{-\sqrt{3}\,\omega z/\xi} \\
&- \sqrt{3}\,(s_{\mathrm{pr}} - \tilde{s})\,\frac{\xi}{\omega}\,\mathrm{e}^{-\sqrt{3}\,\omega z/\xi}\left[\frac{\Delta^2}{4\eta}\left(1 - \mathrm{e}^{-2z/\eta}\right) + \frac{3}{2}\,\mathrm{m}^2\,z \right. \\
&\left. - 3\mathrm{m}\Delta\left(1 - \mathrm{e}^{-z/\eta}\right)\cos\frac{x}{\eta} + \frac{\Delta^2}{2\eta}\left(1 - \mathrm{e}^{-2z/\eta}\right)\cos\frac{2x}{\eta}\right] + \mathcal{O}\left(\varepsilon^2\right) \quad (2.16)
\end{aligned}
$$

$$
\begin{aligned}
\theta(x,z) = \mathrm{m}\,z &+ \Delta\mathrm{e}^{-z/\eta}\cos\frac{x}{\eta} \\
&+ \frac{\xi}{\sqrt{3}\,\omega}\left[h\left(\frac{z}{\xi}\right) - h(0)\right]\left(\mathrm{m} - \frac{\Delta}{\eta}\mathrm{e}^{-z/\eta}\cos\frac{x}{\eta}\right) + \mathcal{O}\left(\varepsilon^2\right), \quad (2.17)
\end{aligned}
$$

where

$$
h(\zeta) = \log\left[s_{\mathrm{pr}} - (s_{\mathrm{pr}} - \tilde{s})\,\mathrm{e}^{-\sqrt{3}\,\omega\zeta}\right] - \frac{(s_{\mathrm{pr}} - \tilde{s})\,\mathrm{e}^{-\sqrt{3}\,\omega\zeta}}{s_{\mathrm{pr}} - (s_{\mathrm{pr}} - \tilde{s})\,\mathrm{e}^{-\sqrt{3}\,\omega\zeta}} \quad (2.18)
$$

determines the tilt angle variation within the boundary-layer. The bulk-asymptotic tilt angle is then given by

$$
\theta(x,z) \approx \theta_{\mathrm{b}}(z) = \frac{\mathrm{m}\,\xi}{\sqrt{3}\,\omega}\left(\log\frac{s_{\mathrm{pr}}}{\tilde{s}} + \frac{s_{\mathrm{pr}} - \tilde{s}}{\tilde{s}}\right) + \mathrm{m}\,z \qquad \text{as} \quad z \gg \eta. \quad (2.19)
$$

We remark that, when $\tilde{s} \neq s_{\mathrm{pr}}$, the leading contribution to $\theta_{\mathrm{b}}(0)$ is independent of Δ, and thus does not depend on the surface roughness. Furthermore, the effective surface tilt angle depends linearly on ξ, which makes it significantly larger than the prediction (2.15), derived with Neumann-like boundary conditions on s, which possesses an extra ξ/η (small) factor. Finally, we remark the fact that $\theta_{\mathrm{b}}(0)$ shares the sign of m if and only if $\tilde{s} < s_{\mathrm{pr}}$. We will return below on the physical origin and implications of this result.

When the induced degree of orientation $\tilde{s}$ does exactly coincide with s_{pr}, all calculations simplify since $h(\zeta) \equiv \log s_{\mathrm{pr}}$, and all first order correction in (2.17) vanish. We therefore push our perturbation analysis, and obtain

$$s(x, z) = s_{\mathrm{pr}} - \frac{s_{\mathrm{pr}}\xi^2}{\omega^2} \left[\mathrm{m}^2 + \frac{\Delta^2}{\eta^2}\mathrm{e}^{-2z/\eta} - \frac{2\mathrm{m}\,\Delta}{\eta}\mathrm{e}^{-z/\eta}\cos\frac{x}{\eta} \right.$$
$$\left. - \mathrm{e}^{-\sqrt{3}\,\omega z/\xi}\left(\mathrm{m}^2 + \frac{\Delta^2}{\eta^2} - \frac{2\mathrm{m}\,\Delta}{\eta}\cos\frac{x}{\eta}\right)\right] + \mathcal{O}\left(\varepsilon^3\right) \qquad (2.20)$$

$$\theta(x, z) = \mathrm{m}\,z + \Delta\,\mathrm{e}^{-z/\eta}\cos\frac{x}{\eta} + \frac{\xi^2}{\omega^2}\left(\frac{2\,\mathrm{m}\,\Delta^2}{\eta}\left(1 - \mathrm{e}^{-2z/\eta}\right)\right.$$
$$\left. - \frac{\Delta^3}{2\,\eta^2}\left(\mathrm{e}^{-z/\eta} - \mathrm{e}^{-3z/\eta}\right)\cos\frac{x}{\eta} - \frac{2\,\mathrm{m}^2\,\Delta}{\eta}z\,\mathrm{e}^{-z/\eta}\cos\frac{x}{\eta}\right) + \mathcal{O}\left(\varepsilon^3\right)\ . \qquad (2.21)$$

Equation (2.21) allows to compute the asymptotic tilt angle θ_{b}, when $\tilde{s} = s_{\mathrm{pr}}$. In fact, once we drop all exponentially-decaying terms in (2.21), we arrive at the interesting result that $\theta_{\mathrm{b}}(z)$ does exactly coincide with (2.14), that is with the expression we derived with a Neumann-like boundary condition on the degree of orientation. In fact, the complete expression (2.21) for the tilt angle $\theta(x, z)$ coincides with (2.12) up to $\mathcal{O}\left(\varepsilon^3\right)$. Thus, any observation on the tilt angle is not able to distinguish among a free and a fixed boundary condition on the degree of orientation, as long as the imposed value $\tilde{s}$ coincides with the preferred value s_{pr}. This similarity between the Neumann and Dirichlet cases can be pursued further. Indeed, we can determine the $\mathcal{O}\left(\varepsilon^2\right)$-contributions in (2.16)-(2.17) also when $\tilde{s} \neq s_{\mathrm{pr}}$. If we then use them to compute the $\mathcal{O}\left(\varepsilon^2\right)$-correction to the asymptotic tilt angle (2.19), we arrive at the following expression, valid at $\mathcal{O}\left(\varepsilon^2\right)$ for any value of $\tilde{s}$:

$$\theta(x, z) \approx \theta_{\mathrm{b}}(z) = \left[\frac{\mathrm{m}\,\xi}{\sqrt{3}\,\omega}\left(\log\frac{s_{\mathrm{pr}}}{\tilde{s}} + \frac{s_{\mathrm{pr}} - \tilde{s}}{\tilde{s}}\right) + \frac{2\,\mathrm{m}\,\xi^2\Delta^2}{\eta\omega^2}\right] + \mathrm{m}\,z \quad \text{as } z \gg \eta, \ (2.22)$$

that yields

$$\theta_{\mathrm{b}}(0) = \frac{\mathrm{m}\,\xi}{\sqrt{3}\,\omega}\left(\log\frac{s_{\mathrm{pr}}}{\tilde{s}} + \frac{s_{\mathrm{pr}} - \tilde{s}}{\tilde{s}}\right) + \frac{2\,\mathrm{m}\,\xi^2\Delta^2}{\eta\omega^2}\ . \qquad (2.23)$$

The $\mathcal{O}\left(\varepsilon^2\right)$-contribution to the effective surface angle $\theta_{\mathrm{b}}(0)$ is thus fully a roughness effect, and does not depend at all on the type of boundary conditions imposed on s. On the other hand, equation (2.23) confirms that the effective surface angle possesses also an $\mathcal{O}\left(\varepsilon\right)$-term when Dirichlet conditions are imposed on the degree of orientation, and $\tilde{s} \neq s_{\mathrm{pr}}$.

Figure 2.3 shows how the degree of orientation varies within the boundary layer, as $\tilde{s}$ is fixed above, equal to, or below s_{pr}. A double boundary-layer structure emerges. All plots exhibit a decrease of s in a region of characteristic size η: this effect comes from the $\mathcal{O}\left(\varepsilon^2\right)$-contribution. A similar surface melting was already presented and

discussed in Figure 2.1. Close to the boundary, the $\mathcal{O}(1)$-term proportional to $(\tilde{s} - s_{\mathrm{pr}})\,\mathrm{e}^{-\sqrt{3}\,\omega z/\xi}$ settles the desired boundary value of s in a thin boundary layer of characteristic size ξ.
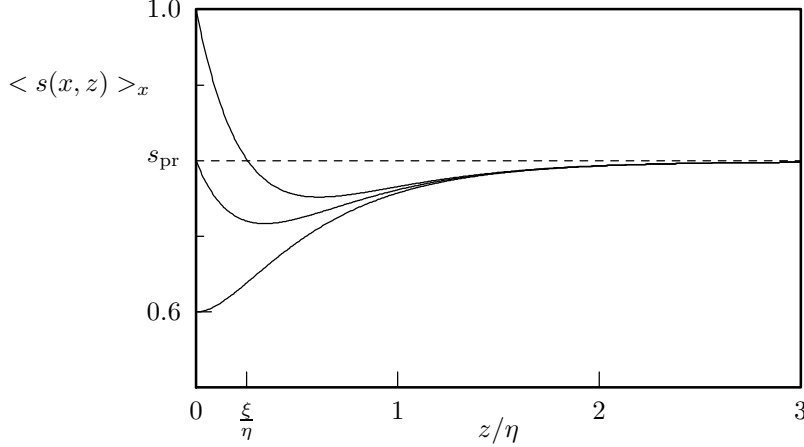

FIG. 2.3. *Boundary layers in the mean degree of orientation* $< s(x,z) >_x$, *when* $\xi = 0.25\eta$, $s_{\mathrm{pr}} = 0.8$, $\omega = 0.6$, $\mathrm{m} = 0.1\eta$, *and* $\Delta = 1.5$, *when Dirichlet-like boundary conditions are applied on the degree of orientation. The boundary degree of orientation* $\tilde{s}$ *is respectively equal to* 1 *(top),* s_{pr} *(middle), and* 0.6 *(bottom).*

3. Effective weak anchoring. Once the boundary layer effects fade away, the main macroscopic effect of a rough surface on the director orientation is to allow for an effective surface tilt angle $\theta_{\mathrm{b}}(0)$, that apparently violates the homeotropic prescription $\theta(0) = 0$ (see (2.15) and (2.23)). It appears then natural to check whether the same macroscopic effect may be modeled through a weak anchoring potential, acting on a smooth surface. In this section we pursue this similarity, and we derive a relation connecting the microscopic roughness parameters with a macroscopic anchoring strength.

To solve the weak-anchoring problem, we consider a nematic liquid crystal which still spreads in the half-space $\mathcal{B} = \{z \geq 0\}$. To better compare our results with classical weak-anchoring models, we settle within Frank's director theory, and thus look for the equilibrium distribution that minimizes the free-energy functional

$$\mathcal{F}[\mathbf{n}] := K \int_{\mathcal{B}} \left|\nabla \mathbf{n}\right|^2 dv + W \int_{\partial \mathcal{B}} f_{\mathrm{w}}[\mathbf{n}]\, da \ . \tag{3.1}$$

The bulk free-energy density in the functional (3.1) can be derived from its order-tensor theory counterpart by setting $s \equiv 1$ in (1.8). The anchoring potential f_{w} is required to attain its minimum at the homeotropic anchoring $\mathbf{n}\big|_{\partial \mathcal{B}} = \mathbf{e}_z$, while W is the *anchoring strength*.

We look again for equilibrium distributions of the type $\mathbf{n}(z) = \sin\theta(z)\,\mathbf{e}_x + \cos\theta(z)\,\mathbf{e}_z$. Thus, the free energy functional (3.1) per unit trasverse area can be written as

$$f[\theta] := K \int \theta'^2(z)\, dz + W f_{\mathrm{w}}\big(\theta(0)\big) \ , \tag{3.2}$$

where we assume $f_{\mathrm{w}}'(0) = 0$ and $f_{\mathrm{w}}''(0) > 0$, in order to guarantee the homeotropic preference. The minimizers of (3.2) satisfy the trivial Euler-Lagrange equation $\theta'' = 0$,

and the boundary condition

$$K\theta'(0) - W f'_{\mathrm{w}}\big(\theta(0)\big) = 0 \ . \tag{3.3}$$

When the anchoring strength W is large enough, the boundary condition (3.3) requires $\theta(0)$ to be small. When this is the case, a Taylor expansion in (3.3) supplies

$$\theta(0) \approx \frac{K\,\mathrm{m}}{W f''_{\mathrm{w}}(0)} = \lambda\,\mathrm{m} \ , \tag{3.4}$$

In (3.4) we have restored the notation $\mathrm{m} = \theta'(0)$ to better compare this estimate with our preceding results, and introduced the *surface extrapolation length*

$$\lambda := \frac{K}{W f''_{\mathrm{w}}(0)} \ , \tag{3.5}$$

a quantity that compares the relative strengths of the elastic and anchoring potentials.

The comparison between (3.4) and our results (2.15)-(2.23) relates the surface extrapolation length to the microscopic roughness parameters and/or the surface value of the degree of orientation. This analogy will be examined in the following section.

4. Discussion. We have examined both the boundary layer structure and the bulk effects of a rough surface bounding a nematic liquid crystal. Our main results may be summarized as follows.

- The roughness of the surface has been modeled by an oscillating anchoring condition, characterized by an oscillation amplitude Δ and a wave length η. Figures 2.1 and 2.3 show that the rough boundary induces a partial melting in a neighborhood (of size η) of the external boundary. When Neumann-like boundary conditions are imposed on the degree of orientation, equation (2.13) quantifies the mean degree of order at the boundary. On the contrary, were s be forced to a prescribed value $\tilde{s}$ on the surface, equations (2.16) and (2.20) show that the boundary condition induces a thin boundary layer, determined by the nematic coherence length ξ.

- Once the degree of orientation decreases, the spatial variations of the tilt angle become cheaper, and thus the θ is keen to steepen close to the external boundary. Figure 2.2 illustrates this effect. As a consequence, the effective boundary tilt angle $\theta_{\mathrm{b}}(0)$, extrapolated from the asymptotic outer solution $\theta_{\mathrm{b}}(z)$, becomes different from the null homeotropic prescription (see equations (2.15) and (2.23)). In the preceding section 3 we have shown that a similar effective anchoring breaking takes place when a weak anchoring potential is assumed on a smooth surface (see equation (3.5) for the characteristic surface extrapolation length). To further pursue this similarity we need to consider separately the different anchorings that may be applied on the degree of orientation.

  - When s is free to choose its boundary value, equation (2.15) shows that the surface extrapolation length is given by

  $$\frac{\lambda}{\xi} = \frac{2\Delta^2}{\omega^2} \frac{\xi}{\eta} + \mathcal{O}\left(\frac{\xi^2}{\eta^2}\right) \ . \tag{4.1}$$

  Thus, the anchoring strength increases when either the roughness amplitude Δ decreases (towards a smooth surface) or the roughness wavelength increases. An estimate of the order of magnitude of the effective

roughness wave-length can be obtained by assuming typical values for the quantities involved in (4.1). Indeed, if we assume $\lambda \approx \xi$, $\Delta \approx 1$, and $\omega \approx \frac{1}{2}$ we arrive at $\eta \approx 10\xi$, that models a roughness wave length in the hundredths of molecular lengths.

– When the boundary conditions fix the value of the degree of orientation at the surface, equation (2.23) yields

$$\frac{\lambda}{\xi} = \frac{1}{\sqrt{3}\,\omega} \left(\log \frac{s_{\mathrm{pr}}}{\tilde{s}} + \frac{s_{\mathrm{pr}} - \tilde{s}}{\tilde{s}} \right) + \frac{2\Delta^2}{\omega^2} \frac{\xi}{\eta} + \mathcal{O}\left(\frac{\xi^2}{\eta^2} \right) . \qquad (4.2)$$

Equation (4.2) shows that the surface extrapolation length includes two quite different contributions. The former depends on the difference between the boundary and the preferred values of the degree of orientation ($\tilde{s}$ and s_{pr}, respectively), while the latter depends on the surface roughness and indeed coincides with (4.1). However, equation (4.2) may lose sense when $\tilde{s} > s_{\mathrm{pr}}$. Indeed, in this case λ may become negative, so providing an *inverse* weak anchoring effect. The physical origin of this odd result may be easily understood if we again resort to the $s^2|\nabla\theta|^2$-term in the free-energy density. By virtue of that term, the tilt angle prefers to limit its spatial variations in regions of higher s. If we force in the surface a higher degree of orientation than the bulk value, the tilt angle will flatten close to the surface, thus exhibiting the opposite behaviour with respect to that shown in Figure 2.2. Equation (4.2) shows that this inverse effect may occur whenever

$$\frac{\tilde{s} - s_{\mathrm{pr}}}{s_{\mathrm{pr}}} \gtrsim \frac{\sqrt{3}\Delta^2}{\omega} \frac{\xi}{\eta} + \mathcal{O}\left(\frac{\xi^2}{\eta^2} \right) . \qquad (4.3)$$

If we again replace the estimates above for Δ, ω, η, we arrive at the result that a fixed degree of orientation is able to completely hide the roughness-induced effective weak anchoring whenever $\tilde{s}$ exceeds s_{pr} by the 10% of the preferred value s_{pr} itself.

REFERENCES

[1] D.W. Berreman: *Solid surface shape and the alignment of an adjacent nematic liquid crystal*. Phys. Rev. Lett. **28** (1972), 1683-1686.

[2] S. Kumar, J.-H. Kim, Y. Shi: *What Aligns Liquid Crystals on Solid Substrates? The Role of Surface Roughness Anisotropy*. Phys. Rev. Lett. **94** (2005), #077803.

[3] F. Batalioto, I.H. Bechtold, E.A. Oliveira, L.R. Evangelista: *Effect of microtextured substrates on the molecular orientation of a nematic liquid-crystal sample*. Phys. Rev. E **72** (2005), #031710.

[4] S. Faetti, M. Gatti, V. Palleschi, T.J. Sluckin: *Almost critical behavior of the anchoring energy at the interface between a nematic liquid crystal and a SiO substrate*. Phys. Rev. Lett. **55** (1985), 1681-1684.

[5] R. Barberi, G.E. Durand: *Order parameter of a nematic liquid-crystal on a rough-surface*. Phys. Rev. A **41** (1990), 2207-2210.

[6] L. Xuan, T. Tohyama, T. Miyashita, T. Uchida. J. Appl. Phys. **96** (2004) 1953-1958. *Order parameters of the liquid crystal interface layer at a rubbed polymer surface*.

[7] G. Barbero, G.E. Durand: *Curvature induced quasi-melting from rough surfaces in nematic liquid-crystals*. J. Physique II **1** (1991), 651-658.

[8] G. Skačej, A.L. Alexe-Ionescu, G. Barbero, S. Žumer: *Surface-induced nematic order variation: Intrinsic anchoring and subsurface director deformations*. Phys. Rev. E **57** (1998), 1780-1788.

[9] V. Mocella, C. Ferrero, M. Iovane, R. Barberi: *Numerical investigation of surface distortion and order parameter variation in nematics*. Liq. Cryst. **26** (1999), 1345-1350.

[10] D.L. Cheung, F. Schmid: *Monte Carlo simulations of liquid crystals near rough walls*. J. Chem. Phys. **122** (2005), #074902.

[11] Y. Sato, K. Sato, T. Uchida: *Relationship between rubbing strength and surface anchoring of nematic liquid-crystal*. Jap. J. Appl. Phys. Lett. **31** (1992), L579-L581.

[12] L.R. Evangelista, G. Barbero: *Theoretical-analysis of actual surfaces - The effect on the nematic orientation*. Phys. Rev. E **48** (1993), 1163-1171.

[13] L.R. Evangelista, G. Barbero: *Walls of orientation induced in sematic-liquid-crystal samples by inhomogeneous surfaces*. Phys. Rev. E **50** (1994), 2120-2133.

[14] A.L. Alexe-Ionescu, R. Barberi, G. Barbero, M. Giocondo: *Anchoring energy for nematic liquid-crystals - Contribution from the spatial variation of the elastic-constants*. Phys. Rev. E **49**, (1994), 5378-5388.

[15] A. Strigazzi: *Surface elasticity and Freedericksz threshold in a nematic cell weakly anchored*. Nuovo Cim. D **10** (1988), 1335-1344.

[16] E.G. Virga: *Variational theories for liquid crystals*. Chapman & Hall, London, UK (1994).

[17] G. Napoli: *Weak anchoring effects in electrically driven Freedericksz transitions*. J. Phys. A: Math. Gen. **39** (2006), 11-31.

[18] M.A. Osipov, T.J. Sluckin, S.J. Cox: *Influence of permanent molecular dipoles on surface anchoring of nematic liquid crystals*. Phys. Rev. E **55** (1997), 464-476.

[19] A.M. Sonnet, E.G. Virga: *Dilution of nematic surface potentials: Statics*. Phys. Rev. E **61** (2000), 5401-5406.

[20] A.M. Sonnet, E.G. Virga, G.E. Durand: *Dilution of nematic surface potentials: Relaxation dynamics*. Phys. Rev. E **62** (2000), 3694-3701.

[21] P.-G. de Gennes, J. Prost: *The Physics of Liquid Crystals* (2nd edition). Ed. Oxford University Press, Oxford, UK (1995).

[22] N. SCHOPOHL and T.J. SLUCKIN. *Defect core structure in nematic liquid crystals*. Phys. Rev. Lett. **59** (1987), 2582-2584.

[23] P. Biscari, G. Guidone Peroli, T.J. Sluckin: *The topological microstructure of defects in nematic liquid crystals*. Mol. Cryst. Liq. Cryst. **292** (1997), 91-101.

[24] P. Biscari, T.J. Sluckin: *Expulsion of disclinations in nematic liquid crystals*. Euro. J. Appl. Math. **14** (2003), 39-59.

[25] P. Biscari, G. Capriz, E.G. Virga: *On surface biaxiality*. Liq. Cryst. **16** (1994), 479-489.

[26] P. Biscari, G. Guidone Peroli: *A hierarchy of defects in biaxial nematics*. Comm. Math. Phys. **186** (1997), 381-392.

[27] M. Holmes: *Introduction to Perturbation Methods*. Ed. Springer-Verlag, New York, USA (1995).

[28] C. Bender, S. Orszag: *Advanced Mathematical Methods for Scientists and Engineers*. Ed. Springer-Verlag, New York, USA (1999).

[29] J. Murdock: *Perturbations. Theory and Methods*. Ed. Wiley-Interscience, New York, USA (1991).

[30] D.R. Smith: *Singular-perturbation theory. An introduction with applications*. Ed. Cambridge University Press, Cambridge, UK (1985).

[31] S. Turzi, PhD Thesis, Politecnico di Milano, Italy, in preparation (2007).